Expanded View Figures

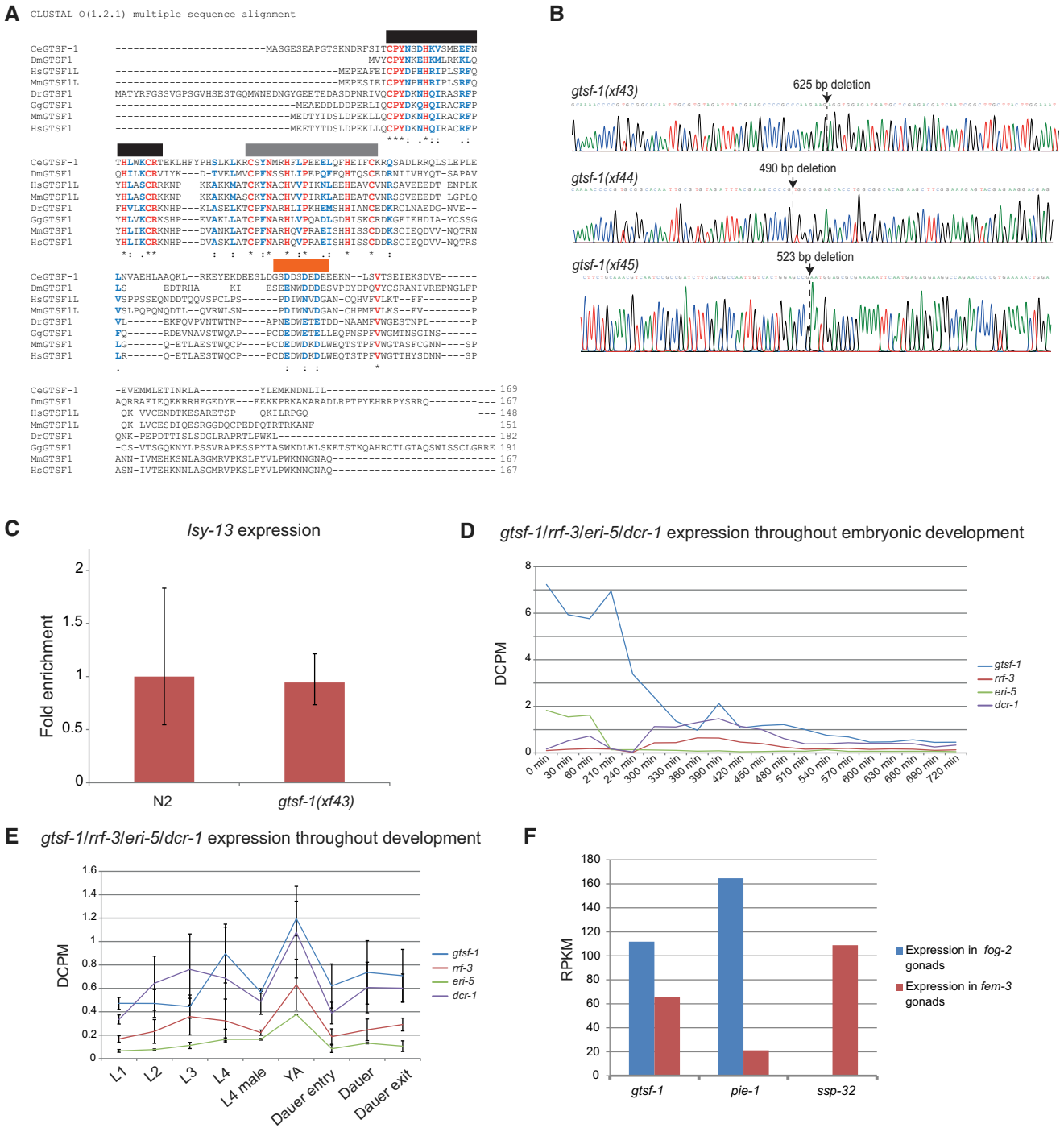

Figure EV1.

◀ **Figure EV1. T06A10.3/CeGTSF-1 is a conserved factor that is expressed during gametogenesis and early development (related to Fig 1).**

A Multiple sequence alignment, using ClustalO, of GTSF-1 and GTSF-1-like proteins. An asterisk and red coloring highlights fully conserved residues. The cysteines and histidines of the CHHC zinc fingers are fully conserved. The first and second CHHC zinc fingers are highlighted with black and gray horizontal bars, respectively. A colon indicates strong conservation of the properties of the residue, while a period indicates weakly conservation of properties. Both cases are also highlighted in blue. Of note, there is a conserved acidic region on the C-terminal tail of GTSF-1, highlighted by an horizontal orange bar. Also, *C. elegans* GTSF-1 has an extended acidic region with more glutamic and aspartic acid residues. Ce, *Caenorhabditis elegans*. Dm, *Drosophila melanogaster*. Mm, *Mus musculus*. Dr, *Danio rerio*. Gg, *Gallus gallus*. Hs, *Homo sapiens*.

B Chromatograms of Sanger sequencing of *gtsf-1* mutant alleles. Deletion sites are indicated with arrows.

C RT–qPCR of *lsy-13* in wild-type and *gtsf-1* mutant embryos. Technical triplicates and biological duplicates were used for this experiment. Error bars represent the standard deviation of two biological replicates. *pmp-3* was used as the normalizing gene.

D mRNA expression profiles of *gtsf-1*, *rrf-3*, *eri-5*, and *dcr-1* during embryonic development. A publicly available Poly-A$^+$ RNA-seq dataset from Boeck *et al* (2016) was used. On the *y*-axis, expression levels are shown in depth of coverage per base per million reads (DCPM).

E *gtsf-1*, *rrf-3*, *eri-5*, and *dcr-1* expression profiles throughout larval development and dauer stage, shown in DCPM. Data points represent average between two Poly-A$^+$ RNA-seq datasets from Boeck *et al*, 2016. Error bars represent the standard deviation of the two replicates.

F Depiction of expression levels of *gtsf-1*, *pie-1* (an oogenic-enriched gene), and *ssp-32* (a spermatogenic-enriched gene), in both *fog-2* mutant gonads (strictly oogenic) and *fem-3* mutant gonads (strictly spermatogenic), as reported in Ortiz *et al*, 2014. Expression is shown in reads per kilobase million (RPKM).

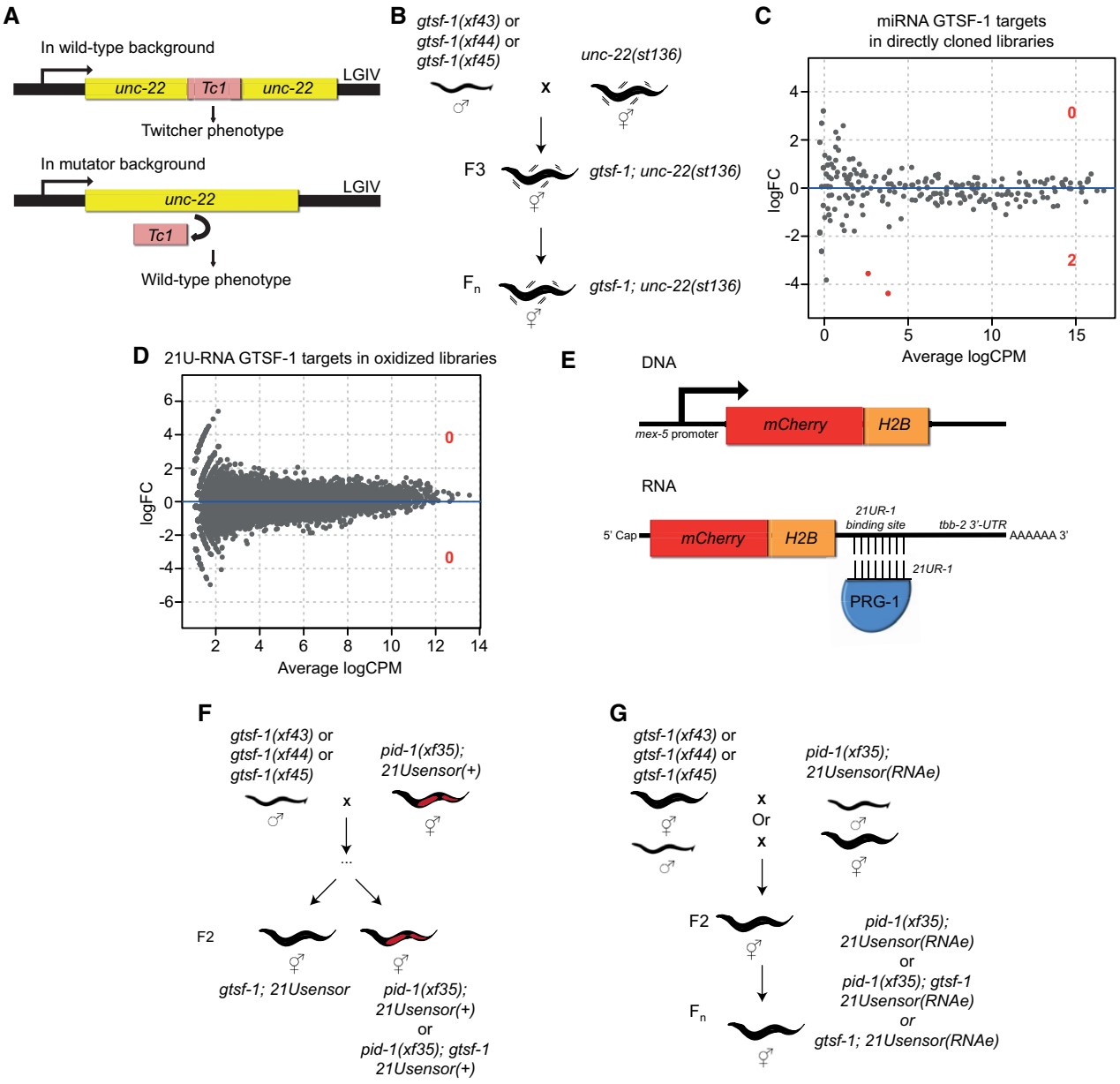

Figure EV2. ***Caenorhabditis elegans*** **GTSF-1 is not involved in TE silencing, the 21U-RNA and miRNA pathways (related to Fig 2).**

A Schematic of the *unc-22(st136)* allele.

B Layout of the *unc-22(st136)* x *gtsf-1* crosses to address transposon derepression. No phenotypic reversions to wild-type were observed in ten replicate *gtsf-1;unc-22 (st136)* populations, grown in parallel for several generations.

C Differential gene expression analysis of miRNAs in wild-type versus *gtsf-1* mutant worms, to address whether miRNAs are globally deregulated in *gtsf-1*. Analysis was performed in the directly cloned libraries, given the higher number of miRNA reads observed. Only two miRNAs (mir-260, mir-262) are significantly downregulated (1% FDR) in *gtsf-1* mutants.

D Differential gene expression analysis of 21U-RNAs in wild-type versus *gtsf-1* mutants. Analysis was performed in the oxidized libraries where a larger number of 21U-RNA reads are found. No significant changes were found at 1% cutoff.

E Overview of the 21Usensor. It consists of an mCherry-histone H2B fusion transgene with a binding site for 21U-R1, an abundant 21U-RNA, in the 3′UTR of the transcript.

F Testing the participation of *gtsf-1* in 21U-RNA-mediated silencing of *C. elegans*. To test this, a non-stably silenced 21Usensor was used, and after crossing with *gtsf-1* mutant animals, the F2 of the indicated genotypes was scored for mCherry expression.

G Schematics of the crosses between *gtsf-1* mutant alleles and an RNAe 21Usensor. No derepression of the 21Usensor was observed in *gtsf-1* mutants in the F2 and in further generations.

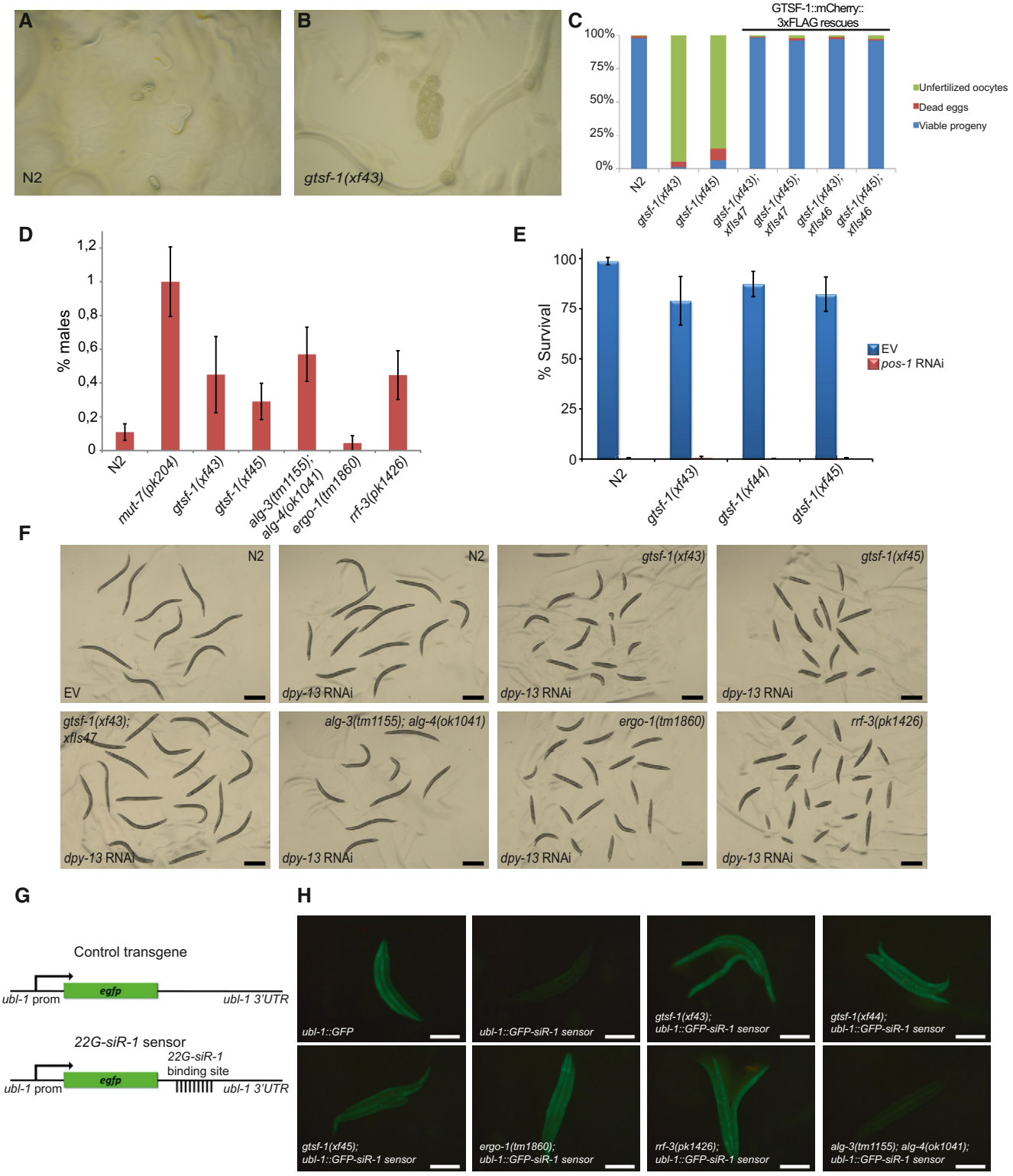

Figure EV3.

Figure EV3. *gtsf-1* animals recapitulate the phenotypes of *alg-3/4* and *ergo-1* mutants (related to Fig 3).

A, B Representative pictures of progenies from synchronized parents of wild-type (A) and *gtsf-1* mutants (B) grown at 25°C. In (A), L1 larvae and gastrulated embryos can be observed, while in (B) only unfertilized oocytes are identified.

C Percentage of dead eggs and unfertilized oocytes laid by wild-type and *gtsf-1* mutant worms when grown at 25°C. These counts were obtained from the same experiment as in Fig 3A. $n = 10$.

D % of males is plotted for the indicated strains. *gtsf-1* mutants show a percentage of males comparable to *alg-3/4* and *rrf-3* mutants, but lower than *mut-7* mutants. Spontaneous male incidence was measured in the progenies of 20 worms. For each plate, percentage of males was calculated and the percentages of the 20 plates were subsequently averaged to obtain the final male percentage value. Error bars represent SEM.

E % Survival of animals of the indicated genotypes on empty vector (EV) and *pos-1* RNAi. Per strain, progenies of $n = 9$–12 worm were scored for embryonic lethality. *gtsf-1* animals respond to *pos-1* RNAi identically to wild type. Error bars represent SD.

F This panel shows a representative fraction of animals from the *dpy-13* RNAi experiment (shown in Fig 3C). Genotypes and treatment with either empty vector (EV) or *dpy-13* RNAi are indicated in the figure. Scale bars represent 0.5 mm.

G Overview of the 22G transgenes. The control transgene consists of GFP controlled by the *ubl-1* promoter and 3′UTR sequences, which allow ubiquitous expression. The 22G-siR-1 sensor is similar to the control transgene except for a binding site for 22G-siR-1 on the 3′UTR that reports on the activity of ERGO-1-dependent 22G-RNAs.

H Genetic requirements for 22G-sensor silencing. Representative fluorescence images of animals carrying 22G-siR-1 sensor combined with other mutations. Scale bars represent 0.5 mm.

Figure EV4. 26G-RNAs are severely depleted in *gtsf-1* mutants (related to Fig 4).

A Venn diagram showing overlap between the 1% FDR GTSF-1 targets defined in the three different NGS library preparation conditions.

B Venn diagram depicting the overlap between the GTSF-1 targets defined in the oxidized and TAP-treated libraries in this study, and NRDE-3 targets as defined elsewhere (Zhou *et al*, 2014).

C–E Exemplary UCSC genome browser tracks with RPM-normalized sRNA coverage profiles. Three biological replicates of wild-type N2 worms (Rep. 1–Rep. 3) and the three *gtsf-1* alleles are shown separately. (C) 22G-RNAs (above) and 26G-RNAs (below) mapping to the 22G-RNA X-cluster. 22G- and 26G-RNA tracks were obtained from TAP-treated and oxidized libraries, respectively. (D, E) 26G-RNA reads mapping to *ssp-16* (D), a sperm-specific family, class P protein, and to *smz-1* (E), a sperm meiosis PDZ domain-containing protein. Directly cloned libraries were used for these tracks.

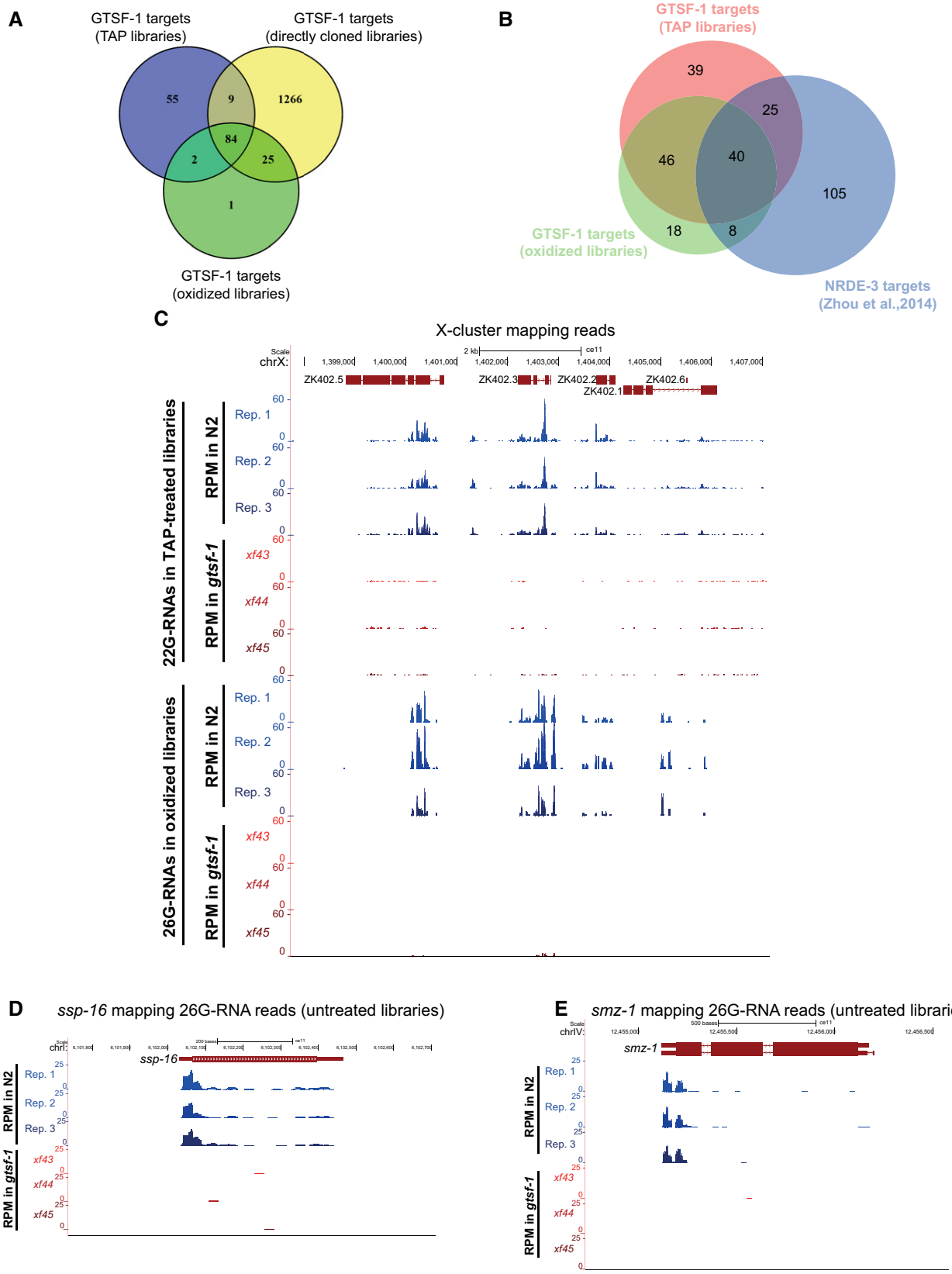

Figure EV4.

Figure EV5. GTSF-1 stably interacts with RRF-3 via its tandem CHHC zinc fingers (related to Figs 5 and 6).

A, B Volcano plots of GTSF-1 IP-mass spectrometry experiments in more stringent wash conditions (600 mM NaCl). Gravid adult worms were used. IPs were performed and measured in quadruplicates. Other than the wash conditions, the setup was identical to Fig 5A and B.

C Brood size count of a 3xFLAG::RRF-3 single-copy transgene. This transgene rescues the fertility defects associated with *rrf-3* mutation almost to a complete extent. Asterisk indicates *P*-value = 0.002185; triple asterisk indicates *P*-value < 0.0001817. *P*-values calculated with Mann–Whitney and Wilcoxon tests, using N2 brood size as a reference. *n* is indicated in the *x*-axis. Horizontal lines represent the median, the bottom and top of the box represent the 25th and 75th percentile. Whiskers include data points that are less than 1.5 × IQR away from the 25th and 75th percentile.

D Overview of *dpy-13* RNAi experiments to worms of the indicated genotypes. A "+" sign indicates that these animals show a normal response to *dpy-13* RNAi, while "+++" animals have an enhanced response to RNAi, having both a more prevalent and stronger *dpy-13* phenotype.

E Western blot analysis of adult animal populations carrying GTSF-1::mCherry::3xFLAG transgenes. Lane 1, Wild-type, non-transgenic worms. Lane 2, WT GTSF-1 protein. Lanes 3 and 4 represent GTSF-1 zinc finger mutants, wherein the zinc finger cysteines are mutated to alanines. The middle, non-labeled lanes are of other GTSF-1 fusion proteins not discussed in this work.

F Wide-field DIC and fluorescence microscopy pictures of worms expressing WT GTSF-1::mCherry::3xFLAG (above) and zinc finger mutant GTSF-1::mCherry::3xFLAG (below). The overall localization of mCherry is not dependent on the zinc fingers. Scale bars indicate 50 μm.

G *In vitro* iCLIP experiment. Purified GTSF-1 protein was incubated with *Caenorhabditis elegans* total RNA from wild-type, UV cross-linked and immunoprecipitated using the GTSF-1 antibody used throughout this study. After the IP, the co-purified RNA was radioactively labeled and the IPs were run on a SDS–PAGE gel followed by membrane transfer. As a positive control, human U2AF65 (hU2AF65) was used (see Sutandy *et al*, 2018). GTSF-1 protein does not associate with RNA beyond background levels. Also, there are not differences between the no antibody, the no cross-link and the no total RNA controls. Same gel is shown, on the left with short exposure and on the right with longer exposure. +* indicates that *gtsf-1(xf43)* total RNA was used, not wild-type. The rationale behind this was that in the *gtsf-1* mutant background, GTSF-1 targets are upregulated. This was expected to increase the iCLIP signal.

Source data are available online for this figure.

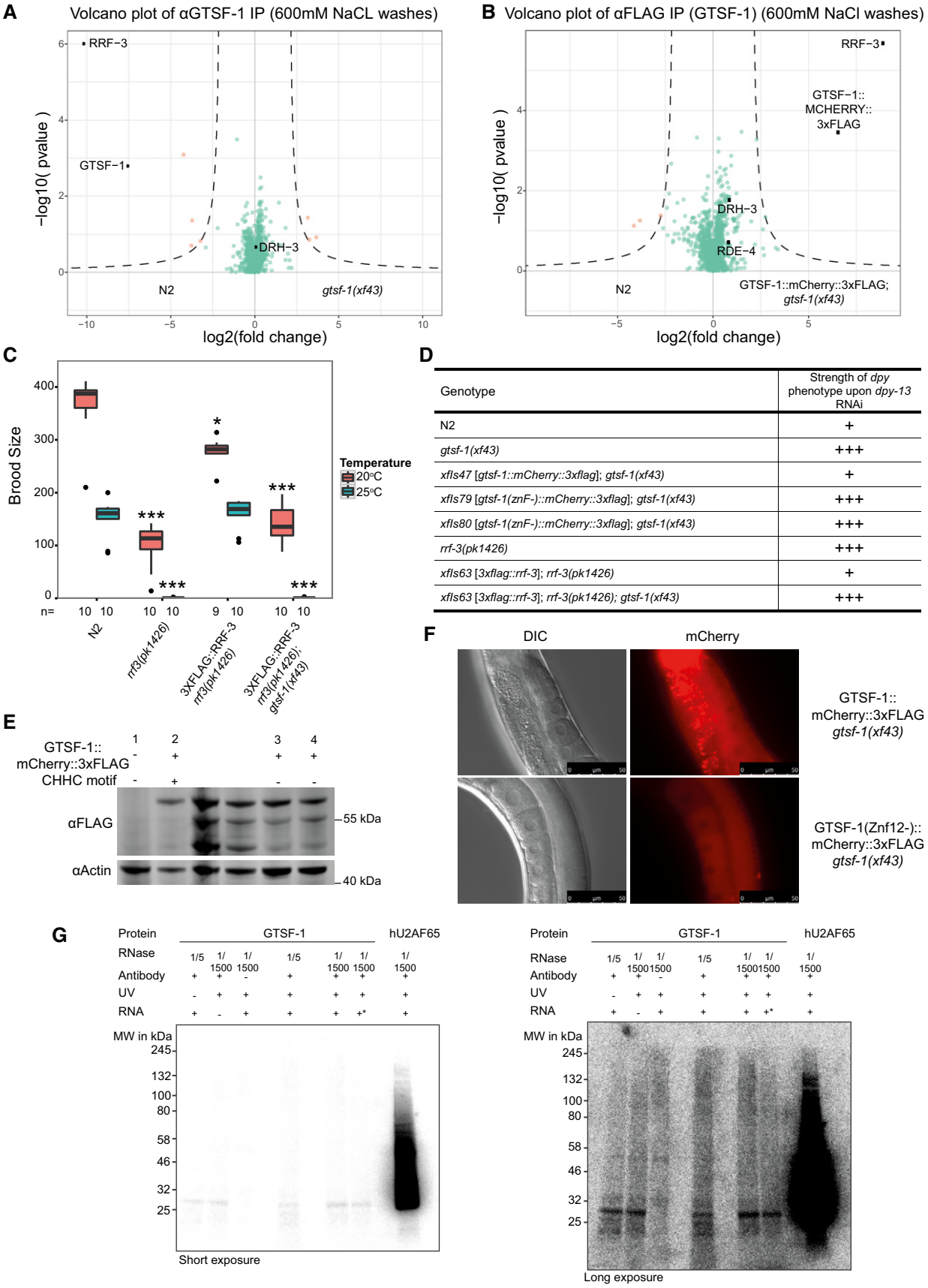

Figure EV5.

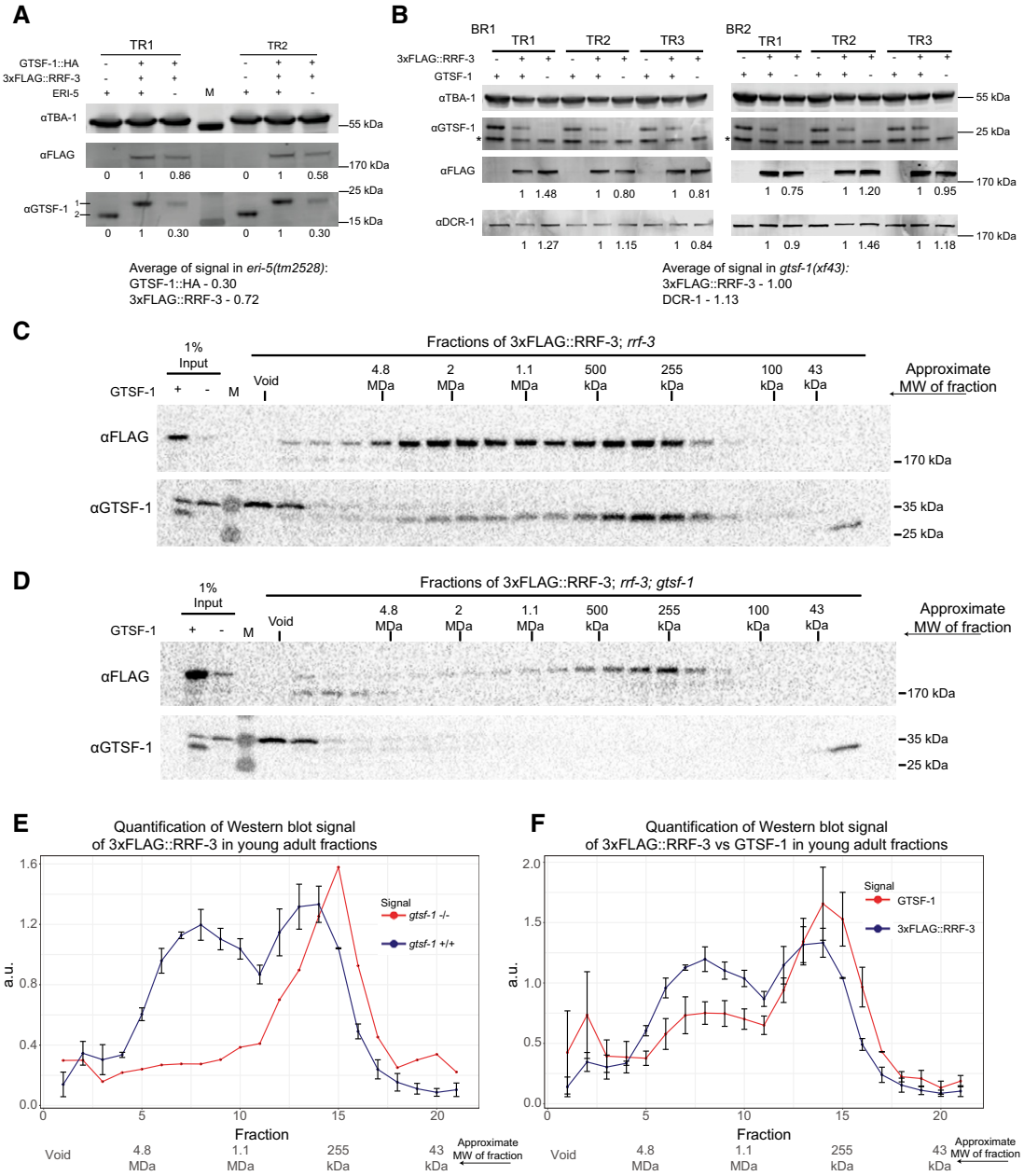

Figure EV6. Stability of ERIC factors in different backgrounds and pre-ERIC/ERIC profiles in young adults (related to Figs 5 and 7).

A Western blot relative quantification of 3xFLAG::RRF-3 and GTSF-1::HA with and without ERI-5. Absence of ERI-5 (–) indicates the presence of *eri-5(tm2528)* deletion allele. Embryonic extracts were used. Double transgenic, wild-type ERI-5 strain was used as the reference. Two technical replicates are shown. For detection, secondary antibodies compatible with LI-COR Odyssey CLx were used. Quantification was done by gating the region surrounding the bands using Image Studio software (v3.1). M, molecular weight marker; TR, technical replicate. For the anti-GTSF-1, 1 represents GTSF-1::HA and 2 represents untagged GTSF-1.

B Relative quantification of Western blot as in (A), but to address the stability of 3xFLAG::RRF-3 and DCR-1 in the absence of GTSF-1 (which indicates the presence of *gtsf-1(xf43)*). Embryonic extracts were used. BR, biological replicate; TR, technical replicate. Asterisk (*) indicates unspecific signal.

C, D Size-exclusion chromatography of 3xFLAG::RRF-3-containing young adult extracts. Fractions were collected, and Western blot was performed for GTSF-1 and 3xFLAG::RRF-3. Fractions collected from extracts with GTSF-1 are shown in (C), and without GTSF-1 are shown in (D). Approximate molecular weight (MW) of the fractions is indicated in the figure. The calculation of these values according to protein standards is shown in the Appendix.

E, F Comparison of size-exclusion chromatography profiles of 3xFLAG::RRF-3 and GTSF-1 in young adult extracts. Relative quantification was performed with the Western blot signal, using ImageJ. Error bars represent standard deviation of two biological replicates, with the exception of 3xFLAG::RRF-3 profile in the absence of GTSF-1 (E), red line. A.u., arbitrary units. (E) Comparison of profiles of 3xFLAG::RRF-3 in the presence of GTSF-1 (blue line) and in the absence of GTSF-1 (red line). (F) Comparison of profiles of 3xFLAG::RRF-3 (blue line) and GTSF-1 (red line).

Source data are available online for this figure.